International Journal of Thermophysics, Vol. 17, No. 4, 1996

Isochoric p–ρ–T Measurements on Difluoromethane (R32) from 142 to 396 K and Pentafluoroethane (R125) from 178 to 398 K at Pressures to 35 MPa

J. W. Magee[1]

Received November 3, 1995

The p–ρ–T relationships were measured for difluoromethane (R32) and pentafluoroethane (R125) by an isochoric method with gravimetric determinations of the amount of substance. Temperatures ranged from 142 to 396 K for R32 and from 178 to 398 K for R125, while pressures were up to 35 MPa. Measurements were conducted on compressed liquid samples. Determinations of vapor pressures were made for each substance. I have used vapor pressure data and the p–ρ–T data to estimate saturated liquid densities by extrapolating each isochore to the vapor pressure, and determining the temperature and density at the intersection. Published p–ρ–T data are in good agreement with this study. For the p–ρ–T apparatus, the uncertainty of the temperature is ± 0.03 K, and for pressure it is $\pm 0.01\%$ at $p > 3$ MPa and $\pm 0.05\%$ at $p < 3$ MPa. The principal source of uncertainty is the cell volume (28.5193 cm^3 at 0 K and 0 MPa), which has a standard uncertainty of ± 0.003 cm^3. When all components of experimental uncertainty are considered, the expanded uncertainty (at the two-sigma level) of the density measurements is estimated to be 0.05%.

KEY WORDS: difluoromethane; pentafluoroethane; p–ρ–T data; saturated liquid; vapor pressure.

1. INTRODUCTION

Current increased technical interest in R32 and R125 has arisen from the fact that these substances or, mixtures containing them are being

[1] Thermophysics Division, Chemical Science and Technology Laboratory, National Institute of Standards and Technology, 325 Broadway, Boulder, Colorado 80303-3328, U.S.A.

0195-928X/96/0700-0803$09.50/0

considered as replacements for R22 and for R502, an azeotropic mixture of R22 and R115. Benchmark measurements of the thermophysical properties of these substances are needed to develop and test predictive models for these properties. Such models will be useful for design calculations for refrigeration processes. Data of the highest accuracy which cover broad ranges of temperature and pressure are needed to develop reliable models of this type. In the last quarter of 1993, McLinden et al. [1] reviewed the existing thermophysical property data for various refrigerants, including R32 and R125. More recently, Outcalt and McLinden [2] have analyzed the available data for R32 and R125 and developed a modified Benedict–Webb–Rubin equation of state for each fluid; the present data were used in the development of these equations.

In the following discussion, some of the key studies of densities and vapor pressures of R32 and R125 are referenced. For liquid and gaseous R32, Defibaugh et al. [3] measured densities from 242 to 373 K at pressures to 6.5 MPa, and Holste [4] measured densities from 150 to 375 K at pressures to 72 MPa. For liquid and supercritical gaseous states for R125, Defibaugh and Morrison [5] measured densities from 275 to 369 K at pressures to 6.3 MPa, Holste [6] measured densities from 180 to 350 K at pressures to 68 MPa, and Wilson et al. [7] measured densities from 198 to 448 K at pressures to 10 MPa. For gaseous R125, Boyes and Weber [8] measured densities from 293 to 363 K at pressures to 4.5 MPa.

Densities of the saturated liquid and vapor pressures have been reported by other investigators. Such data are used to anchor a model for the thermophysical properties to the saturation boundary. For R32, vapor pressures have been reported by Weber and Goodwin [9] from 208 to 237 K, by Holcomb et al. [10] from 295 to 349K, by Defibaugh et al. [3] from 268 to 351 K, and by Malbrunot et al. [11] from 191 to 348 K. Also, for R32, saturated liquid densities have been reported by Holcomb et al. [10] from 295 to 347 K, by Defibaugh et al. [3] from 243 to 338 K, and by Higashi et al. [12] from 336 to 351 K. For R125, vapor pressures have been reported by Weber and Silva [13] from 219 to 335 K, by Holste [6] from 220 to 338 K, and by Monluc et al. [14] from 303 to 339 K. Also, for R125, Defibaugh and Morrison [5] reported saturated liquid densities from 276 to 338 K. In summary, p–ρ–T data in the saturated and compressed liquid phases for these substances are scarce, especially at temperatures below 273 K.

In this paper, I report new p–ρ–T measurements for R32 and R125 at temperatures ranging from just above T_{tr} to a maximum temperature near 400 K. I also report new vapor pressure measurements and saturated liquid densities for these substances.

2. MEASUREMENTS

2.1. p–ρ–T Apparatus and Procedures

The apparatus used in this work has been used for studies of both pure fluids and mixtures. Since details of the apparatus are available in previous publications [15, 16], they are only briefly reviewed here. An isochoric technique was employed to measure the single-phase liquid densities in this study. In this method, a sample of fixed mass is confined in a container of nearly fixed volume. The volume of the container is accurately known as a function of pressure and temperature. The temperature is changed in selected increments, and the pressure is measured at each temperature, until the upper limit of either temperature (400 K) or pressure (35 MPa) is attained. When an isochore is completed, that is, after the upper temperature or pressure limit of the run has been reached, the sample is expanded into a light-weight stainless steel cylinder which is immersed in liquid nitrogen. When the p–ρ–T cell and its connecting capillary have been heated to about 20 K above the critical temperature of the sample, the cylinder is sealed. warmed to ambient temperature, and weighed. The density of the test fluid is then determined from a knowledge of the cell volume and of the mass difference of the steel cylinder before and after trapping the sample. Allowances to account for the noxious volumes in the system, such as those of the capillaries and the pressure gauge, are made for each point. A small adjustment to the apparent sample mass was made to account for the change in atmospheric buoyant force acting on the steel cylinder. The density of the sample fluid is then the quotient of the number of moles and the volume of the cell at each pressure and temperature.

The sample cell is a cylindrical piece of electrolytic tough pitch copper containing a cavity with a volume of approximately 28.5 cm^3. It is suspended inside an evacuated cryostat from a thin-walled stainless-steel tube used for reflux cooling. High-resistance wire wound tightly around the cell is used to heat the cell. The cell temperature is determined with a platinum resistance thermometer (calibrated at NIST relative to the IPTS-68, with temperatures converted to the ITS-90) embedded in a small well at the top of the cell. An ultrastable current source supplies the thermometer with a current of 2 mA and is equipped with relays capable of reversing the direction of current in the circuit. Errors caused by steady-state thermal and contact EMFs are minimized by averaging voltages measured for opposite directions of current flow. The temperatures were controlled and reproduced within 1 mK. The total uncertainty in the temperature ranged from 10 mK at 100 K to 30 mK at 400 K.

Pressures are measured by reading the period of vibration, averaged over 10 s, of an oscillating quartz crystal transducer which is connected to the sample cell through a fine-diameter (0.2-mm-i.d.) capillary. Since the frequency of the transducer varies with temperature, the transducer has been anchored in an insulated aluminum block controlled at 333.15 ± 0.05 K. The transducer has been calibrated with an oil-lubricated piston gauge, accurate within $\pm 0.01\%$. Calibrations have demonstrated that the transducer is extremely stable over long periods of time. Changes of less than 0.003% were observed over 1 year. The expanded uncertainty in the pressure measurements is approximately 0.01% for pressure greater than 3 MPa but increases to 0.05% at low pressures (1 MPa and lower) as a result of the transducer resolution, of the fluctuations in the temperature of the pressure transducer, and of the occasional hysteresis in the vibrational frequency of the quartz element.

2.2. Samples

High-purity samples were obtained for the measurements. The sample of R32 had the highest purity, 0.9994 mole fraction. The largest impurity was CF_3CH_3 (R143a) with a mole fraction of 0.0004. Other impurities included 100 ppm of CH_3Cl, 10 ppm of $CHCl_2F$, and 5 ppm of H_2O. The purity of the R125 sample was 0.99736 mole fraction. The largest impurity was CF_3CClF_2 with a mole fraction of 0.00263. Other impurities included 2.0 ppm of CO_2, 0.4 ppm of CO, and 1.44 ppm of H_2O. Although the water content of each of these samples was very small, the samples were loaded into thoroughly dried and evacuated cylinders which contained molecular sieves. Subsequent analysis revealed less than 1 ppm of H_2O remaining.

2.3. Assessment of Uncertainties

For the p–ρ–T apparatus the uncertainty in temperature is ± 0.03 K and is a combination of the ice-point (R_0) resistor drift, temperature gradients in the cell enclosure, the drift of the 10-Ω standard resistor used in the PRT circuit, and radiation from the head of the thermometer or from the lead wires to cooler surfaces in their vicinity.

The uncertainty in pressure is $\pm 0.01\%$ at $p > 3$ MPa and $\pm 0.05\%$ at $p < 3$ MPa. The higher uncertainty at $p < 3$ MPa is due to the increasing contribution of the variation with temperature of the ratio of the periods

of vibration in vacuum and at pressure (τ_0/τ) of the oscillating quartz crystal pressure transducer, given by

$$p = C[(t - Dt^2) + (1 - 2Dt)\,\delta t] \tag{1}$$

where C and D are constants, the variable t is defined as $t = 1 - (\tau_0/\tau)^2$, τ is the period at pressure p, τ_0 is the period in vacuum, the fluctuation of transducer temperature about its setpoint is $\delta T = 333.15 - T(\mathrm{K})$, the corresponding fluctuation in the variable t is $\delta t = -2(\tau_0/\tau^2)\,\delta\tau_0$, and $\delta\tau_0$ is the change in τ_0 due to δT given by $\delta\tau_0 = (d\tau_0/dT)\,\delta T$. The coefficients obtained by calibration are $(d\tau_0/dt) = 0.2113\ \mathrm{ns \cdot K^{-1}}$, $C = -3.4926892968275 \times 10^2$ MPa, and $D = 3.5484565468152 \times 10^{-2}$. Starting with the manufacturer's working equation, this scheme was developed to correct (to a first order approximation) for the temperature dependence of the transducer period of oscillation. Its contribution to the pressure derived from Eq. (1) becomes appreciable in the lower 5% of the full-scale (70 MPa) range of the instrument.

The uncertainty in the experimental values of density is due primarily to the uncertainties in the volume of the sample cell and in the determination of the mass of substance contained in the experimental volume. Before this study, methane gas was used to determine the cell volume [17]. The mean ideal volume was 28.5193 $\mathrm{cm^3}$ (extrapolated to 0 K and 0 MPa) with an uncertainty of $\pm 0.003\ \mathrm{cm^3}$ ($\pm 0.01\%$). The results were confirmed (within $0.0009\ \mathrm{cm^3}$) by determinations with nitrogen gas. With an allowance for the cross terms, $\delta T\, dV_{\mathrm{cell}}/dT$ and $\delta p\, dV_{\mathrm{cell}}/dp$, arising from uncertainties in measured temperatures and pressures, the estimated uncertainty of the cell volume is approximately $\pm 0.0045\ \mathrm{cm^3}$ ($\pm 0.015\%$). The sample mass determinations have an uncertainty of $\pm 2 \times 10^{-3}$ g. The effect of sample purity on the measurements could be more pronounced for the R125 samples due to the presence of a 0.00263 mole fraction of R115 impurity. In this work, however, I report specific density values which are only weakly affected by similar chemical species which solidify at temperatures above 77 K. Due to the substitution of a chlorine atom for a hydrogen atom, the molecular mass of R115 is approximately 30% higher than R125; thus, the mixture's molar mass is raised by about 0.07%. If molar densities are to be calculated from specific density values for R125 from this work, then a mixture molar mass should be used for the conversion. The effect of the impurity on the vapor pressure measurements is negligibly small due to the similar boiling points of R115 and R125. Combining the uncertainty of the measured amount of sample with the uncertainty of the cell volume, it is estimated that the values of density have an expanded uncertainty of $\pm 0.05\%$.

3. RESULTS

3.1. p–ρ–T Results

The experimental temperatures, pressures, and densities for liquid R32 are presented in Table I; for R125 the results are presented in Table II. These tables also present calculated densities using the modified Benedict–Webb–Rubin equation of state developed by Outcalt and McLinden [2] and the deviations of the calculated densities from the experimental values. The original temperature measurements were made on the IPTS-68 scale and were converted to ITS-90 using a published table of conversions [18]. To illustrate the range of measurements for each of the fluids, the isochoric data for liquid R32 and R125 are plotted in Figs. 1 and 2.

Comparisons of the isochoric p–ρ–T measurements with an equation of state for each substance has been facilitated by the recent study of Outcalt and McLinden [2], who have presented new correlations for R32 and for R125. These correlations are based, in part, on the results of this study along with selected data sets from other laboratories. Outcalt and McLinden graphically depicted each of the deviations of the calculated density from the experimental density for these selected data and the results of this study. Their comparisons show that there is consistent agreement ($\pm 0.15\%$) for liquid R32 densities from Defibaugh and Morrison [3] and Holste [4] with this study. For liquid R125, at temperatures below 300 K, the liquid densities of Defibaugh and Morrison [5], Holste [6], and Wilson et al. [7] are clearly in good agreement with this study within $\pm 0.2\%$. In the supercritical region, however, it is not possible to ascertain how well published densities agree with this study. In this region, small experimental pressure differences produce large differences in density due to the magnitude of the derivative in the expression $\Delta P(\partial\rho/\partial P)_T$.

3.2. Densities of the Saturated Liquid

Saturated liquid densities derived in this study were obtained by extrapolating the isochoric data to their intersection with the vapor pressure equation presented by Outcalt and McLinden [2]. The accuracy of the extrapolation depends primarily on the difference in the slope of the experimental isochore and the vapor pressure curve. At the high densities of this work, the uncertainty of the temperature intersection is approximately ± 0.01 K. This leads to about $\pm 0.10\%$ in the estimated density of the saturated liquid, including the estimated experimental uncertainty of,the density measurement. The results of the saturated liquid density extrapolations are presented in Table III for R32 and in Table IV

Table I. Experimental p–ρ–T Data for Difluoromethane (R32): T, Temperature (ITS-90); p, Pressure; ρ_{exp}, Density; and ρ_{calc} from Ref. 2; Dev. = 100 $(\rho_{calc} - \rho_{exp})/\rho_{exp}$

T (K)	P (MPa)	ρ_{exp} (kg·m^{-3})	ρ_{calc} (kg·m^{-3})	Dev. (%)
142.000	5.494	1419.5	1419.8	0.02
144.000	10.929	1419.0	1419.0	0.00
145.999	16.441	1418.6	1418.4	−0.01
148.000	21.961	1418.2	1417.8	−0.02
149.999	27.462	1417.8	1417.2	−0.04
151.999	32.947	1417.4	1416.7	−0.05
151.999	3.872	1394.6	1394.6	0.00
153.999	5.964	1391.3	1391.5	0.01
155.999	10.955	1390.8	1390.8	0.00
158.000	16.002	1390.4	1390.2	−0.02
159.999	21.048	1390.0	1389.6	−0.03
161.998	26.088	1389.7	1389.1	−0.04
163.999	31.102	1389.3	1388.5	−0.06
160.000	4.299	1375.3	1375.7	0.02
161.999	8.985	1374.8	1374.9	0.01
164.000	13.772	1374.4	1374.3	−0.01
166.000	18.566	1374.0	1373.7	−0.02
168.000	23.358	1373.7	1373.2	−0.04
169.999	28.139	1373.3	1372.7	−0.05
171.999	32.887	1373.0	1372.1	−0.06
170.000	3.822	1350.6	1350.9	0.02
174.000	9.802	1346.9	1346.9	0.00
175.999	14.187	1346.5	1346.4	−0.01
177.999	18.584	1346.2	1345.9	−0.02
180.000	22.974	1345.8	1345.4	−0.04
181.999	27.342	1345.5	1344.9	−0.05
183.999	31.698	1345.2	1344.4	−0.06
183.999	5.946	1318.5	1318.6	0.01
186.000	9.920	1318.1	1318.1	0.00
187.999	13.931	1317.7	1317.6	−0.01
190.000	17.947	1317.4	1317.1	−0.02
192.000	21.951	1317.1	1316.6	−0.03
194.000	25.946	1316.8	1316.2	−0.04
196.000	29.921	1316.5	1315.7	−0.05
198.000	33.886	1316.2	1315.3	−0.06
198.001	5.687	1283.3	1283.4	0.01
199.999	9.252	1282.9	1282.9	0.00
202.000	12.849	1282.6	1282.4	−0.01
203.999	16.441	1282.3	1282.0	−0.02
206.000	20.034	1282.0	1281.6	−0.03
208.000	23.611	1281.7	1281.2	−0.04
210.000	27.178	1281.4	1280.8	−0.04

Table I. *(Continued)*

T (K)	P (MPa)	ρ_{exp} (kg·m^{-3})	ρ_{calc} (kg·m^{-3})	Dev. (%)
212.001	30.735	1281.1	1280.4	−0.05
213.998	34.276	1280.8	1280.0	−0.06
209.999	4.248	1250.6	1250.7	0.01
212.000	7.449	1250.2	1250.2	−0.01
214.002	10.694	1249.9	1249.7	−0.01
216.000	13.934	1249.6	1249.4	−0.02
217.999	17.182	1249.3	1249.0	−0.03
220.000	20.424	1249.0	1248.6	−0.03
222.001	23.654	1248.7	1248.3	−0.04
224.000	26.878	1248.5	1247.9	−0.04
226.000	30.092	1248.2	1247.6	−0.05
228.000	33.291	1247.9	1247.2	−0.06
224.000	4.228	1213.5	1213.5	0.00
226.002	7.089	1213.1	1213.0	−0.01
228.001	9.979	1212.8	1212.6	−0.01
229.999	12.871	1212.5	1212.3	−0.02
232.000	15.765	1212.2	1212.0	−0.02
234.000	18.655	1211.9	1211.6	−0.03
235.998	21.537	1211.7	1211.3	−0.03
238.000	24.418	1211.4	1211.0	−0.03
239.999	27.289	1211.2	1210.7	−0.04
242.000	30.153	1210.9	1210.4	−0.04
244.002	33.008	1210.7	1210.1	−0.05
238.002	4.141	1174.4	1174.7	0.03
239.999	6.680	1174.0	1174.2	0.02
242.001	9.248	1173.7	1173.9	0.01
243.999	11.819	1173.4	1173.6	0.01
246.000	14.383	1173.2	1173.2	0.01
248.000	16.952	1172.9	1172.9	0.00
250.001	19.515	1172.7	1172.7	0.00
251.999	22.070	1172.4	1172.4	0.00
254.000	24.623	1172.2	1172.1	−0.01
256.000	27.170	1172.0	1171.8	−0.01
257.999	29.712	1171.7	1171.6	−0.01
260.001	32.248	1171.5	1171.3	−0.02
262.000	34.774	1171.3	1171.0	−0.02
254.002	5.883	1132.5	1132.4	−0.01
256.000	8.136	1132.2	1132.1	−0.01
258.002	10.396	1131.9	1131.8	−0.02
260.001	12.658	1131.7	1131.5	−0.02
262.000	14.919	1131.4	1131.2	−0.02
263.999	17.172	1131.2	1130.9	−0.02
266.000	19.427	1131.0	1130.7	−0.03
268.000	21.678	1130.7	1130.5	−0.03
270.001	23.922	1130.5	1130.2	−0.03
272.000	26.162	1130.3	1130.0	−0.03

Table I. *(Continued)*

T (K)	P (MPa)	ρ_{exp} (kg·m^{-3})	ρ_{calc} (kg·m^{-3})	Dev. (%)
274.001	28.401	1130.1	1129.7	−0.03
276.000	30.632	1129.9	1129.5	−0.03
277.999	32.859	1129.7	1129.2	−0.04
279.998	35.076	1129.4	1129.0	−0.04
273.998	6.889	1073.9	1074.0	0.01
277.998	10.665	1073.4	1073.4	0.00
282.000	14.446	1073.0	1072.9	0.00
285.999	18.214	1072.5	1072.4	−0.01
290.001	21.980	1072.1	1072.0	−0.01
294.000	25.732	1071.7	1071.6	−0.01
297.999	29.473	1071.3	1071.2	−0.01
302.001	33.200	1070.9	1070.7	−0.02
290.001	7.119	1021.3	1021.4	0.00
294.000	10.329	1020.9	1020.9	0.00
298.001	13.545	1020.5	1020.4	−0.01
302.002	16.762	1020.1	1020.0	−0.01
306.002	19.974	1019.7	1019.6	−0.01
310.000	23.180	1019.3	1019.3	−0.01
314.001	26.369	1019.0	1018.8	−0.01
318.001	29.571	1018.6	1018.5	−0.01
321.999	32.748	1018.2	1018.1	−0.01
309.999	5.249	932.4	932.7	0.03
313.999	7.672	932.0	932.2	0.02
317.999	10.108	931.7	931.8	0.01
322.001	12.551	931.3	931.4	0.01
326.001	14.992	931.0	931.0	0.01
329.999	17.439	930.6	930.7	0.01
334.001	19.887	930.3	930.4	0.01
338.001	22.332	930.0	930.0	0.01
342.002	24.777	929.6	929.7	0.01
346.001	27.217	929.3	929.3	0.00
350.001	29.642	929.0	928.9	−0.01
354.000	32.073	928.7	928.5	−0.02
358.000	34.505	928.4	928.2	−0.02
348.002	6.815	710.9	712.2	0.19
351.999	8.002	710.6	711.3	0.10
356.001	9.203	710.4	710.7	0.05
360.000	10.415	710.1	710.2	0.02
364.000	11.638	709.9	709.9	0.00
368.000	12.867	709.6	709.6	−0.01
372.000	14.103	709.4	709.3	−0.02
376.001	15.345	709.2	709.0	−0.03
379.999	16.591	708.9	708.7	−0.03
384.001	17.842	708.7	708.4	−0.04
388.000	19.095	708.4	708.1	−0.04
392.000	20.350	708.2	707.8	−0.05
395.999	21.607	708.0	707.5	−0.06

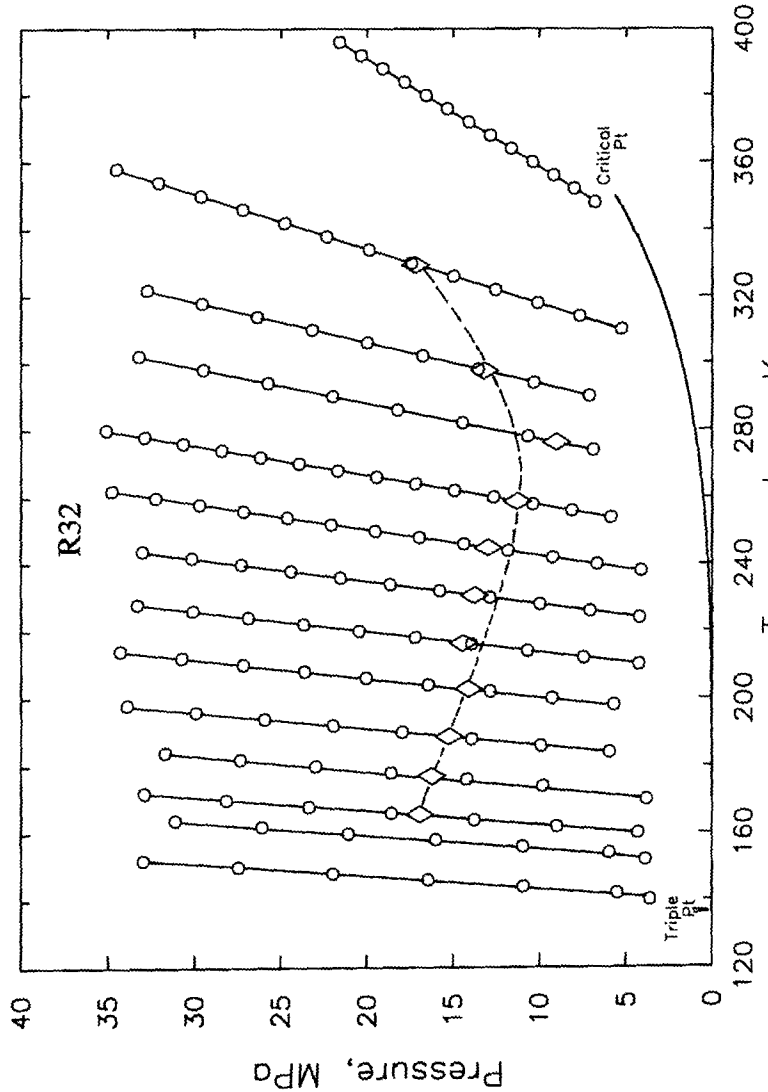

Fig. 1. Range of p–ρ–T measurements (○) for liquid difluoromethane (R32) and inflection points (◇) defined by $(\partial^2 p/\partial T^2)_\rho = 0$.

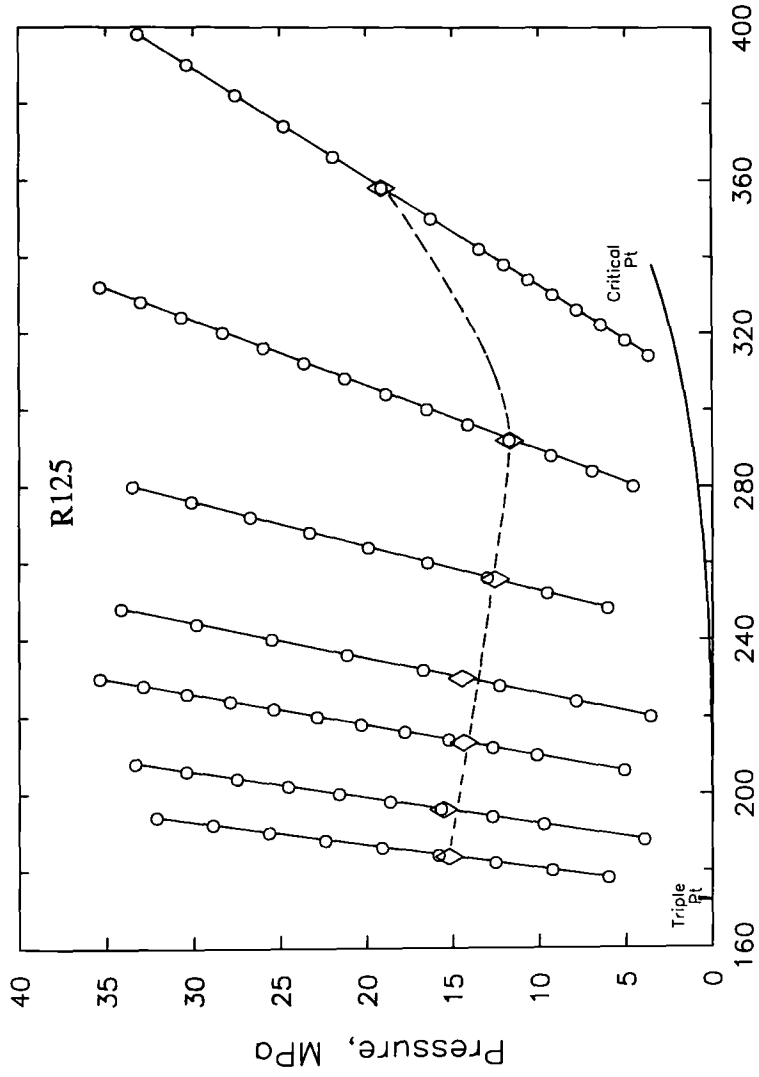

Fig. 2. Range of p–ρ–T measurements (○) for liquid pentafluoroethane (R125) and inflection points (◇) defined by $(\partial^2 p/\partial T^2)_\rho = 0$.

Table II. Experimental p–ρ–T Data for Pentafluoroethane (R125): T, Temperature (ITS-90); p, Pressure; ρ_{exp}, Density; and ρ_{calc} from Ref. 2; Dev. = 100 $(\rho_{calc} - \rho_{exp})/\rho_{exp}$

T (K)	P (MPa)	ρ_{exp} (kg·m^{-3})	ρ_{calc} (kg·m^{-3})	Dev. (%)
178.000	6.012	1683.7	1683.9	0.01
180.001	9.259	1683.1	1683.1	0.00
182.000	12.536	1682.6	1682.4	−0.01
184.000	15.826	1682.1	1681.8	−0.02
186.001	19.109	1681.7	1681.3	−0.02
188.001	22.385	1681.3	1680.9	−0.03
190.002	25.655	1680.9	1680.5	−0.03
192.000	28.904	1680.6	1680.1	−0.03
194.001	32.147	1680.2	1679.8	−0.03
188.000	3.931	1648.8	1649.1	0.02
192.001	9.737	1647.4	1647.4	0.00
194.000	12.703	1647.0	1646.8	−0.01
196.000	15.673	1646.6	1646.3	−0.01
198.000	18.643	1646.2	1645.9	−0.02
200.000	21.606	1645.8	1645.5	−0.02
202.000	24.559	1645.4	1645.1	−0.02
204.001	27.505	1645.1	1644.8	−0.02
205.999	30.429	1644.7	1644.4	−0.02
208.000	33.353	1644.4	1644.1	−0.02
206.001	5.107	1593.6	1593.6	0.00
210.000	10.149	1592.6	1592.4	−0.01
212.000	12.695	1592.2	1591.9	−0.02
214.000	15.243	1591.8	1591.4	−0.02
216.000	17.786	1591.5	1591.0	−0.03
217.999	20.322	1591.1	1590.7	−0.03
219.999	22.851	1590.8	1590.3	−0.03
221.999	25.374	1590.4	1589.9	−0.03
223.998	27.893	1590.1	1589.6	−0.03
226.000	30.406	1589.8	1589.3	−0.03
228.000	32.906	1589.5	1588.9	−0.04
230.001	35.396	1589.2	1588.6	−0.04
220.000	3.584	1543.2	1543.0	−0.01
223.999	7.888	1542.0	1541.6	−0.03
228.000	12.303	1541.2	1540.6	−0.04
232.000	16.711	1540.5	1539.8	−0.04
236.000	21.108	1539.9	1539.1	−0.05
240.000	25.487	1539.2	1538.4	−0.05
244.001	29.846	1538.7	1537.8	−0.06
248.000	34.173	1538.1	1537.1	−0.06
248.001	6.081	1453.4	1452.8	−0.04
252.001	9.523	1452.6	1451.9	−0.05
256.002	12.978	1452.0	1451.1	−0.06

Table II. *(Continued)*

T (K)	P (MPa)	ρ_{exp} (kg · m^{-3})	ρ_{calc} (kg · m^{-3})	Dev. (%)
260.000	16.431	1451.4	1450.5	−0.06
263.998	19.872	1450.8	1449.9	−0.06
267.998	23.300	1450.2	1449.2	−0.07
271.998	26.722	1449.7	1448.7	−0.07
275.999	30.126	1449.2	1448.1	−0.08
279.999	33.511	1448.7	1447.5	−0.08
279.999	4.587	1318.3	1317.9	−0.04
284.001	6.952	1317.6	1317.0	−0.04
288.001	9.331	1317.0	1316.4	−0.05
292.001	11.714	1316.5	1315.8	−0.06
296.001	14.100	1316.0	1315.2	−0.06
300.002	16.484	1315.5	1314.7	−0.06
304.002	18.866	1315.0	1314.2	−0.06
308.002	21.236	1314.5	1313.6	−0.07
311.999	23.608	1314.1	1313.2	−0.07
316.001	25.974	1313.6	1312.7	−0.07
320.001	28.340	1313.2	1312.2	−0.07
323.998	30.695	1312.7	1311.8	−0.07
327.999	33.034	1312.3	1311.3	−0.07
332.001	35.372	1311.8	1310.9	−0.07
313.999	3.684	1123.1	1122.4	−0.06
318.000	5.051	1122.5	1121.7	−0.07
322.001	6.432	1121.9	1121.2	−0.07
326.001	7.823	1121.5	1120.7	−0.07
330.000	9.220	1121.1	1120.1	−0.08
334.002	10.622	1120.6	1119.6	−0.09
338.000	12.025	1120.3	1119.1	−0.11
342.001	13.436	1119.9	1118.6	−0.12
350.002	16.262	1119.1	1117.6	−0.13
358.000	19.091	1118.3	1116.7	−0.14
366.000	21.921	1117.6	1115.9	−0.15
374.001	24.747	1116.8	1115.1	−0.15
382.000	27.568	1116.1	1114.4	−0.15
389.998	30.378	1115.3	1113.8	−0.14
398.001	33.181	1114.6	1113.2	−0.12

for R125. Outcalt and McLinden [2] fitted saturated liquid densities, including these results, to a six-coefficient ancillary equation. The densities calculated with this equation are also presented in Tables III and IV. The deviations of the experimental densities from the values calculated from the equation are depicted in Fig. 3 for R32 and in Fig. 4 for R125. At the temperature which overlaps the study by Holcomb et al. [10] (304.726 K),

Table III. Saturated Liquid Density of Difluoromethane (R32): T, Temperature (ITS-90); $\rho_{sat,exp}$, Saturated Liquid Density; and $\rho_{sat,calc}$, Saturated Liquid Density Calculated from Ref. 2; Dev. = 100 $(\rho_{sat,exp} - \rho_{sat,calc})/\rho_{sat,exp}$

T (K)	$\rho_{sat,exp}$ (kg·m^{-3})	$\rho_{sat,calc}$ (kg·m^{-3})	Dev. (%)
138.86	1423.0	1423.2	−0.016
150.51	1395.9	1395.1	0.055
158.20	1375.7	1376.4	−0.050
168.43	1351.4	1351.2	0.017
179.80	1322.6	1322.7	−0.005
194.08	1286.1	1286.2	−0.003
207.43	1251.0	1251.0	−0.003
221.17	1213.8	1213.7	0.005
234.18	1176.9	1177.1	−0.012
248.94	1133.2	1133.4	−0.016
266.68	1078.0	1077.2	0.077
282.46	1022.2	1022.4	−0.011
304.73	933.0	932.9	0.009

Table IV. Saturated Liquid Density of Pentafluoroethane (R125): T, Temperature (ITS-90); $\rho_{sat,exp}$, Saturated Liquid Density; and $\rho_{sat,calc}$, Saturated Liquid Density Calculated from Ref. 2; Dev. = 100 $(\rho_{sat,exp} - \rho_{sat,calc})/\rho_{sat,exp}$

T (K)	$\rho_{sat,exp}$ (kg·m^{-3})	$\rho_{sat,calc}$ (kg·m^{-3})	Dev. (%)
173.48	1688.2	1688.5	−0.019
184.70	1653.1	1652.6	0.030
201.27	1597.8	1597.9	−0.005
216.84	1544.1	1544.4	−0.020
240.73	1457.1	1456.7	0.026
273.04	1321.5	1231.2	0.026
308.46	1124.9	1123.9	0.091

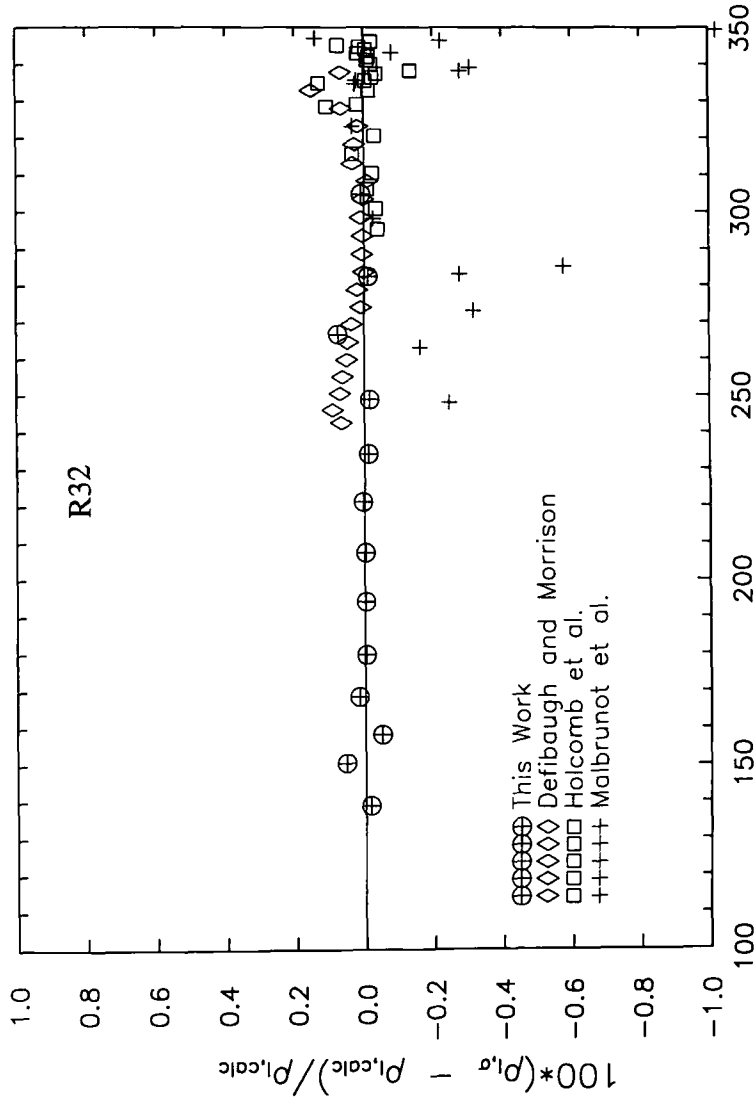

Fig. 3. Percentage deviations of the experimental saturated liquid densities for difluoromethane (R32) obtained in this work (⊕), by Defibaugh and Morrison [3] (◇), by Holcomb et al. [10] (□), and by Malbrunot et al. [11] (+) from the values calculated with the ancillary equation of Outcalt and McLinden [2].

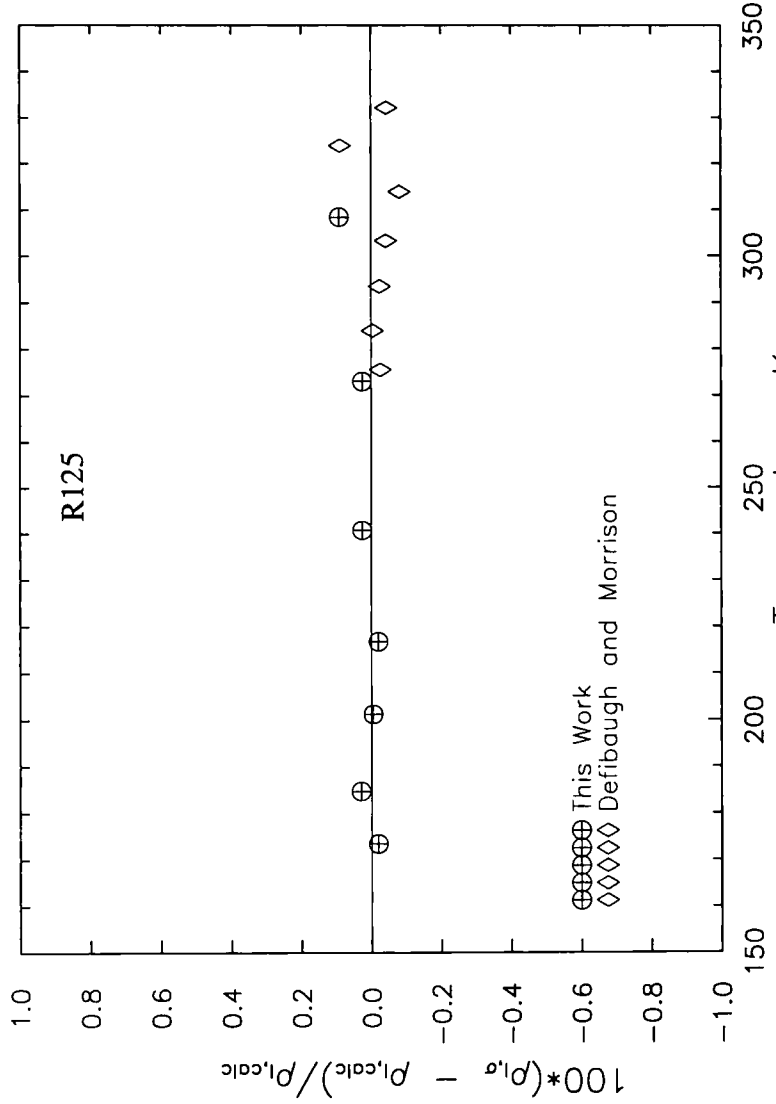

Fig. 4. Percentage deviations of the experimental saturated liquid densities for pentafluoroethane (R125) obtained in this work (⊕) and by Defibaugh and Morrison [5] (◇) from the values calculated with the ancillary equation of Outcalt and McLinden [2].

the agreement of their results with this study is ±0.02%. In the region of overlap for R125 (273–308 K); the agreement of this work with that of Defibaugh and Morrison is between ±0.05 and ±0.15%. This agreement is also acceptable since it falls within the combined uncertainties of the two data sets.

3.3. Vapor Pressures

During the course of the density determinations, measurements of the vapor pressure were performed for the pure substances. To carry out these measurements, the apparatus was modified slightly by adding a vacuum tight manifold consisting of two pressure transducers which were separated by valves. The transducers were of the same type used in the p–ρ–T measurements but had ranges of 0–0.2 and 0–6 MPa. Before this work, each transducer was calibrated with a gas-lubricated piston gauge whose pressure values have an expanded uncertainty of 0.005%. Special care was taken to exclude air from the cell, when the samples were charged. The samples were charged at a temperature slightly below room temperature. Then, the sample was heated to a temperature about 0.1 K below its critical point. A portion of the sample was released until the pressure had fallen to about the critical pressure. Then the sample was cooled to a temperature slightly below the triple point. Then the vapor space above the sample was vacuum pumped to remove any volatile impurities which remained. The sample was then heated to a temperature about 5 K above the triple point. Then, alternately, the vapor pressure was measured followed by a brief cycle of vacuum pumping on the vapor space. After temperature equilibrium was reachieved, the measured pressure was the same as for the previous measurement. Three such cycles were carried out. Thus, I verified that the level of volatile impurities is below the measurement threshold.

Table V. Experimental p_{sat} Data for Difluoromethane (R32): T, Temperature (ITS-90); $p_{sat,exp}$, Vapor Pressure; and $p_{sat,calc}$, Vapor Pressure Calculated from Ref. 2; Dev. = 100 $(p_{sat,exp} - p_{sat,calc})/p_{sat,exp}$

T (K)	$p_{sat,exp}$ (kPa)	$p_{sat,calc}$ (kPa)	Dev. (%)
270.00	733.80	734.22	−0.056
280.00	1005.7	1007.1	−0.132
290.00	1348.7	1350.3	−0.117
300.00	1772.9	1774.9	−0.116
310.00	2291.1	2293.3	−0.095
320.00	2916.7	2919.4	−0.091
330.00	3665.6	3669.5	−0.104

The measured temperatures and pressures are given in Table V for R32 and in Table VI for R125. The expanded uncertainty of the reported vapor pressures is estimated to be $\pm 0.1\%$. The deviations given in the tables are those from the ancillary equations reported by Outcalt and McLinden [2].

Table VI. Experimental p_{sat} Data for Pentafluoroethane (R125): T, Temperature (ITS-90); $p_{sat,exp}$, Vapor Pressure; and $p_{sat,calc}$, Vapor Pressure Calculated from Ref. 2; Dev. $= 100\ (p_{sat,exp} - p_{sat,calc})/p_{sat,exp}$

T (K)	$p_{sat,exp}$ (kPa)	$p_{sat,calc}$ (kPa)	Dev. (%)
180.00	5.758	5.682	1.338
190.00	12.484	12.400	0.680
200.00	24.673	24.688	−0.063
205.00	33.821	33.817	0.014
210.00	45.499	45.509	−0.021
215.00	60.216	60.256	−0.067
220.00	78.553	78.595	−0.054
224.00	96.212	96.241	−0.031
225.00	101.09	101.11	−0.016
226.00	106.11	106.16	−0.047
230.00	128.33	128.41	−0.065
235.00	161.12	161.18	−0.036
240.00	200.06	200.10	−0.016
245.00	245.78	245.90	−0.052
250.00	299.11	299.36	−0.085
250.00	299.00	299.36	−0.119
255.00	360.98	361.26	−0.078
260.00	432.12	432.43	−0.072
265.00	513.07	513.72	−0.126
270.00	605.32	606.01	−0.113
275.00	709.60	710.22	−0.086
280.00	826.84	827.30	−0.055
285.00	957.73	958.24	−0.053
290.00	1103.5	1104.1	−0.057
295.00	1265.3	1266.0	−0.054
300.00	1443.5	1445.0	−0.101
305.00	1640.9	1642.4	−0.092
310.00	1858.2	1859.7	−0.080
315.00	2096.0	2098.1	−0.103
320.00	2356.0	2359.6	−0.152
325.00	2643.0	2645.9	−0.107
330.00	2956.1	2959.3	−0.107
335.00	3297.6	3302.9	−0.162

3.4. Inflection Points

Magee and Kobayashi [19] have discussed methods for determining the locus of isochoric inflection points from compressed-gas and liquid p–ρ–T measurements. Because each p–ρ–T inflection point is defined by $(\partial^2 P/\partial T^2)_\rho = 0 = -\rho^2/T(\partial C_v/\partial \rho)_T$, it is the state condition where the isochoric heat capacity has an extremum. The locus of such inflection points maps the state conditions where a density change results in no change in the energy storage per mole. At a fixed temperature, the sign of the derivative $(\partial C_v/\partial \rho)_T$ changes at the locus of inflections. This is a fundamental molecular property which is closely tied to the interactions of molecules in a condensed phase, where molecular packing is sufficient for neighboring molecules to affect one another. The inflection points are plotted in Fig. 1 for R32 and Fig. 2 for R125.

4. CONCLUSIONS

For difluoromethane (R32), I have reported 136 p–ρ–T state conditions, 13 saturated liquid densities, and 7 vapor pressures. For pentafluoroethane (R125), I have reported 77 p–ρ–T state conditions, 7 saturated liquid densities, and 33 vapor pressures. The uncertainty of pressure is $\pm 0.05\%$, that of density is $\pm 0.05\%$, and that of temperature is ± 0.03 K. For saturated liquid densities, agreement with published values of comparable uncertainty was $\pm 0.15\%$. This falls within the combined uncertainty of the results.

ACKNOWLEDGMENTS

I am grateful to John Howley for his important technical contributions to the experimental measurements. I thank Stephanie Outcalt and Mark McLinden for generous technical assistance with the calculations and many helpful discussions during this study. I acknowledge the financial support of the Air Conditioning and Refrigeration Technology Institute. I have profitted from many discussions with W. M. Haynes, Gerald Straty, and Marcia Huber.

REFERENCES

1. M. O. Mclinden, M. L. Huber, and S. L. Outcalt, *Proceedings, ASME Winter Meeting*, New Orleans LA, Nov. 28–Dec. 3 (1993), Paper No. 93-WA/HT-29.
2. S. L. Outcalt and M. O. Mclinden, *Int. J. Thermophys.* **16**:79 (1995).
3. D. R. Defibaugh, G. Morrison, and L. A. Weber, *J. Chem. Eng. Data* **39**:333 (1994).

4. J. C. Holste, Texas A&M University, private communication to W. M. Haynes, NIST.
5. D. R. Defibaugh and G. Morrison, *Fluid Phase Equil.* **80**:157 (1992).
6. J. C. Holste, *Thermodynamic Properties of Refrigerants R-125 and R-141b*, Final report to ASHRAE on project RP-654 (1993).
7. L. C. Wilson, W. V. Wilding, G. M. Wilson, R. L. Rowley, V. M Felix, and T. Chilsom-Carter, *Fluid Phase Equil.* **80**:167 (1992).
8. S. J. Boyes and L. A. Weber, *J. Chem. Thermodyn.* **27**:163 (1995).
9. L. A. Weber and A. R. H. Goodwin, *J. Chem. Eng. Data* **38**:254 (1993).
10. C. D. Holcomb, V. G. Niesen. L. J. VanPoolen, and S. L. Outcalt. *Fluid Phase Equil.* **91**:145 (1993).
11. P. F. Malbrunot, P. A. Meunier, G. M. Scatena, W. H. Mears, K. P. Murphy, and J. V. Sinka, *J. Chem. Eng. Data* **13**:16 (1967).
12. Y. Higashi, H. Imaizumi, and S. Usuba, *13th Japan. Symp. Thermophys. Prop.* (1992), p. 65.
13. L. A. Weber and A. M. Silva, *J. Chem. Eng. Data* **39**:808 (1994).
14. Y. Monluc, T. Sagawa, H. Sato, and K. Watanabe, *12th Japan. Symp. Thermophys. Prop.* (1991), p. 65.
15. R. D. Goodwin, *J. Res. Natl. Bur. Stand. (US)* **65C**:231 (1961).
16. J. W. Magee and J. F. Ely, *Int. J. Thermophys.* **9**:547 (1988).
17. J. W. Magee, W. M. Haynes, and M. J. Hiza, submitted for publication (1995).
18. H. Preston-Thomas, *Metrologia* **27**:3 (1990).
19. J. W. Magee and R. Kobayashi, in *Proceedings, 8th Symposium on Thermophysical Properties Vol. 1*, J. V. Sengers, ed. (ASME, New York, 1982), p. 321.